The Influence of Inlet Asymmetry on Steam Turbine Exhaust Hood Flows

Zoe Burton *
School of Engineering
and Computing Sciences
Durham University
South Road, Durham
DH1 3LE
Email: zoe.burton@durham.ac.uk

Simon Hogg
School of Engineering
and Computing Sciences
Durham University
South Road, Durham
DH1 3LE
Email: simon.hogg@durham.ac.uk

Grant L. Ingram
School of Engineering and Computing Sciences
Durham University
South Road, Durham
DH1 3LE
Email: g.l.ingram@durham.ac.uk

ABSTRACT

It has been widely recognized for some decades that it is essential to accurately represent the strong coupling between the last stage blades (LSB) and the diffuser inlet, in order to correctly capture the flow through the exhaust hoods of steam turbine low pressure cylinders. This applies to any form of simulation of the flow i.e. numerical or experimental. The exhaust hood flow structure is highly three-dimensional and appropriate coupling will enable the important influence of this asymmetry to be transferred to the rotor. This however presents challenges as the calculation size grows rapidly when the full annulus is calculated. The size of the simulation means researchers are constantly searching of methods to reduce the computational effort without compromising solution accuracy. However, this can result in excessive computational demands in numerical simulations. Unsteady full-annulus CFD calculation will remain infeasible for routine design calculations for the foreseeable future. More computationally efficient methods for coupling the unsteady rotor flow to the hood flow are required that bring computational

*Address all correspondence to this author.

expense within realisable limits whilst still maintaining sufficient accuracy for meaningful design calculations. Research activity in this area is focused on developing new methods and techniques to improve accuracy and reduce computational expense. A novel approach for coupling the turbine last stage to the exhaust hood employing the non-linear harmonic (NLH) method is presented in this paper. The generic, IP free, exhaust hood and last stage blade geometries from Burton et.al. [1], that are representative of modern designs, are used to demonstrate the effectiveness of the method. This is achieved by comparing results obtained with the NLH to those obtained with a more conventional mixing-plane approach. The results show that the circumferential asymmetry can be successfully transferred in both directions between the exhaust hood flow and that through the LSB, by using the NLH. This paper also suggests that for exhaust hoods of generous axial length, little change in C_p is observed when the circumferential asymmetry is captured. However, the predicted flow structure is significantly different which will influence the design and placement of the exhaust hood internal 'furniture'.

Nomenclature

C_p Static Pressure Recovery Coefficient

k Periodic Fluctuation Index

M Number of Perturbations

N Number of Harmonics per Perturbation

n Number of Blades per Row

P Pressure

t Time

U Conservative Flow Variable

U_n Variable for RMS calculation

$\vec{r}$ Position Vector

V Relative Velocity

α Swirl Angle

δ Pressure Difference at Interface Plane

θ Cell Count in Theta Direction

Subscripts

d Downstream

P Static Pressure (for RMS)

P_{dyn} Dynamic Pressure (for RMS)

P_t Total Pressure (for RMS)

T Total/Stagnation

t Tangential

u Upstream

r,t,z Velocity Components

1 Hood/Diffuser Inlet

2 Hood Outlet

Superscripts

$\bar{}$ Time Mean

Abbreviations

BPF Blade Passing Frequency

CFD Computational Fluid Dynamics

CFL Courant Freidrichs Levy

EDS Exhaust Design System

IP Intellectual Property

LSB Last Stage Blades

NLH Non-Linear Harmonic

RMS Root Mean Square

1 Introduction

The amount by which the static pressure at exit from the last stage of a LP steam turbine differs from the condenser pressure is a function of the pressure recovery in the diffuser and the losses in the exhaust hood. Under ideal conditions, all of the kinetic energy in the flow leaving the last stage blades would be recovered as an increase in static pressure through the diffuser and all exhaust hood losses would be negligible. These conditions correspond to an exhaust hood static pressure recovery coefficient of unity (C_p = 1) and result in the minimum static pressure at exit from the last stage and therefore maximum turbine power output. In reality, only part of the kinetic energy in the flow leaving the last stage is recovered in the diffuser and there will be some losses in the exhaust hood. C_p values for real LP exhausts are therefore less than unity and often negative in value e.g. [2] where C_p = -0.25.

It is widely recognized that the flow distribution exiting from the last stage turbine blades has an important impact of the flow through the diffuser and exhaust hood. It is essential to accurately capture the coupling between the exit flow from the last stage and the diffuser inlet flow, in order to achieve representative flow through the exhaust hood and to determine reliable values for exhaust hood performance parameters such as static pressure recovery coefficient. This statement applies equally to experiments and calculations. Experiments, even at significantly reduced model scales, are in general too complex and expensive for manufacturers to use them explicitly within their design processes. Full three-dimensional, unsteady, compressible, whole annulus computational fluid dynamics (CFD) calculations are also still prohibitively expensive for adoption into routine design calculations. This has resulted in research workers proposing a wide range of numerical approaches in

recent years, that are aimed at reducing the computational demand whilst maintaining sufficiently accurate results. No single 'best-practice' methodology has so far emerged from this work.

The simplest approach to coupling the last stage to the exhaust hood is through separate stand alone last stage and exhaust hood calculations, where the rotor blade exit flow from the stage calculation is used to provide the diffuser inlet flow boundary condition in the exhaust hood calculation. This couples the rotor flow to the exhaust hood flow in just one direction i.e. the rotor flow can influence the hood flow, but not in reverse. Accurate simulation of the flow through LP exhausts requires the coupling to be captured in both directions in the calculations.

Of the fully coupled calculation methodologies that have been proposed to date, the most advanced are those which transfer the circumferential asymmetry of the exhaust hood flow to the rotor as well as that radial flow distribution. The exhaust hood flow asymmetry is due to the non axis-symmetric geometry and the swirl velocity field from the rotation of the turbine blades. It is believed that asymmetry has an important influence on the flow structure within the diffuser [3].

The mixing plane approach is a computational efficient method of capturing the interaction [4], however the circumferential averaging at the rotor exit/hood inlet mixing plane, removes the circumferentially non-uniform inlet flow. Mixing planes are used widely in turbomachinery calculations and they provide a computational efficient method for coupling stationary and rotating frames in a single steady flow calculation. Flow conditions are circumferentially averaged across a mixing-plane and so only radial variations in flow quantities are transmitted between frames. The mixing plane approach is not ideal for LP exhaust hood calculations due to the need to also transmit information on circumferential variations between the rotor and exhaust hood calculations domains. As discussed earlier it is important to capture the asymmetry of the rotor exit/diffuser inlet flow in the calculation. The approaches used by other workers for achieving this fall into three categories. These are; frozen rotor method, full unsteady calculations and custom industry developed tools.

The Frozen Rotor approach is the most widely adopted method of capturing the exhaust hood inlet circumferential asymmetry [5–7]. This approach can essentially be viewed as a simplification that removes the time-dependence from CFD simulations, reducing 3-D, unsteady turbomachinery calculations to steady flow predictions. If this type of method is used to calculate LP exhaust flows, it is necessary to include all of the rotor blade passages in the calculation as a minimum, to ensure suitable periodicity. As a result calculations are still computationally expensive, typically featuring cell counts of order 50 million [5] and lengthy convergence times e.g. 267 hours [7]. The frozen rotor approach is therefore still too expensive for use by manufacturers in their design tools [5].

The continual improvements in computer hardware and software design that fuels the growth in available computing power, has now made full 3-D, unsteady LP exhaust hood calculations a realistic option for validation type calculations [6, 8–10]. Unsteady studies have shown that the turbine blades not only experience high frequency fluctuations due to the stator rotor interaction, but also low frequency forces due to the interaction between the stage and the exhaust hood [6]. The amplitude of the fluctuations caused by the rotor/hood interaction frequencies are larger than that for the stator/rotor interaction [8]. The unsteady effects can become particularly prominent under off-design operating conditions [9]. Full 3-D, unsteady exhaust flow calculations are, by their nature, significantly more expensive than frozen rotor calculations. It is possible to perform calculations of this type, but available computing power is still some way from where it needs to be in

order for this approach to be manageable for design calculations.

The third category of published LP exhaust calculation methodology allowing for circumferential flow asymmetry in the coupling between the rotor exit flow and the diffuser inlet flow, are industry developed tools that incorporate the companys own bespoke coupling methods. One example is Exhaust Design System (EDS). This was developed in the mid 1990's [3] and has been adopted by Alstom in their in-house 3-D exhaust design tool [11, 12]. The method involves first building up a bank of periodic last stage calculations over a wide range of exit pressures. The exhaust hood is calculated in a separate steady calculation. The rotor exit flow is coupled to the diffuser inlet flow in an iterative manner. The diffuser inlet is divided circumferentially into a number of discrete sectors. As the hood calculation progresses the 3-D hood flow produces circumferential variations in the flow structure in the diffuser inlet region The boundary conditions on the diffuser inlet plane are adjusted by selecting the rotor exit flow for each sector that best matches the local diffuser inlet conditions predicted in the exhaust hood calculation. The diffuser inlet boundary condition is progressively updated by iterating in this manner until the 3-D exhaust hood calculation has converged. The advantage of this approach is that it is computationally much less demanding than the other approaches described earlier in this section. The bank of stage calculations only needs to be done once. When this is available, different exhaust hoods can be investigated with the same last stage blade design by simply modifying the exhaust hood calculation, without any need to revisit the last stage blade calculations.

A new approach for coupling the flow through the LP last stage blades to the exhaust hood using the non-linear harmonic method is described in this paper. This allows the stage and hood flow to be solved in a single calculation. The computational cost is much lower than frozen rotor or full 3-D unsteady calculations yet it retains the important advantage over mixing-plane calculations of coupling both circumferential and radial flow variations in both direction across the rotor/hood interface plane. The results obtained with the new approach are bench-marked against calculations carried out with a mixing-plane, in order to quantify the impact of the improved coupling including circumferential effects on the flow structure and exhaust hood losses.

2 Non-Linear Harmonic Method

The non-linear harmonic (NLH) method was developed by He and Ning [13] to enable quasi-unsteady flow calculations to be carried out at a fraction of the computational cost of traditional full 3-D unsteady calculations.

The fundamental assumption of the NLH method is that the most dominant unsteady disturbances are caused by the relative rotation of the blade rows i.e. the blade passing frequency (BPF) in the relative frame of reference for each blade row. With this in mind, an unsteady flow variable can be decomposed into a time-averaged component, and the sum of the unsteady periodically appearing perturbations, equation 1.

$$U(\vec{r},t) = \bar{U}(\vec{r}) + \sum U'(\vec{r},t) \tag{1}$$

Each periodic perturbation can be decomposed into its fundamental frequency and N harmonics by Fourier transformation, according to equation 2. This means that only one blade passage needs to be modelled as the frequencies can be reconstructed around the full annulus. The number of perturbations, M, that need to be modelled when calculating the flow through a blade passage is determined by the number of important blade passing frequencies acting at the blade row inlet and exit boundaries. The accuracy of the solution is controlled by the order of the Fourier series, i.e. modelling an infinite number of harmonics will give the equivalent result to the sliding mesh calculation. In this way, each perturbation can be modelled by a limited number of sinusoidal harmonic oscillations, which are integer multiples of the first harmonic of each blade passing frequency.

$$U'(\vec{r},t) = A_{U,k}\cos(k\omega t) + B_{U,k}\sin(k\omega t) \tag{2}$$

Substitution of equation 2 into equation 1 leads to:

$$U(\vec{r},t) = \bar{U}(\vec{r}) + \sum^{M}\sum^{N} A_{U,k}\cos(k\omega t) + B_{U,k}\sin(k\omega t) \tag{3}$$

The value of the instantaneous flow variable, U, in equation 3 is a direct function of the number of perturbations and the number of frequencies per perturbation, N, calculated. These are user specified variables in the calculation as discussed in Section 3.2.2. Substitution of equation 3 into the Reynolds Averaged Navier-Stokes equations and collecting all same order sine and cosine terms, results in $2N$ time-invariant coupled equations being formed for each perturbation. These additional equations represent the influence of the deterministic unsteady fluctuations on the mean flow field, in an analogous manner to the way that the Reynolds Stress terms represent the influence of turbulence on the mean flow. The total number of coupled steady equations that have to be solved for each flow variable, U, including the mean flow equation, therefore becomes $2MN+1$, where M is the number of perturbations modelled for the blade passage flow.

Although the NLH approach is significantly less computationally demanding than full annulus unsteady methodologies, it is more computationally demanding than steady single passage calculations such as the mixing plane approach for the reasons explained above. The improved accuracy of modelling additional harmonics must be balanced against the additional computational demand required to solve the extra transport equations associated with them.

The method used to pass flow information across the stator to rotor and the rotor to exhaust hood interface planes is described in detail by Vilmin [14]. The NLH approach requires just one blade passage to be calculated for both the stator and the rotor blade rows. The harmonic equations resulting from the Fourier decomposition are periodic in space with phase-lagged frequency components. This allows the time-averaged flow to be reconstructed around the annulus on either

side of the interfaces, even though only one blade passage has been calculated. Good continuity can be achieved across the interfaces provided that a high enough number of harmonics is included in the calculation. It is normally recommended that at least three harmonic frequencies are included when calculating turbomachinery stage flows.

The NLH method is ideally suited to LP exhaust hood calculations including the last stage blades. Flow gradients will be much larger in the radial direction compared to the circumferential direction at exit from the last stage. Capturing the circumferential variations in the time-averaged flow by calculating variations at just the fundamental passing frequencies and a limited number of their harmonics, has the potential to capture much more of the flow physics, without needing to go the the expense of full annulus 3-D blade row calculations.

3 Computational Methods

This paper presents the results from two computational fluid dynamics (CFD) calculations on a coupled steam turbine exhaust hood and LSB system. The NLH method has not previously been used to capture the interaction. The importance of the inlet circumferential asymmetry will be assessed by comparing results from the NLH approach with the mixing plane approach, which only captures the radial variations at the rotor exit/diffuser inlet calculation interface.

3.1 Grid Generation

3.1.1 Last Stage Blades

The last stage blade geometry used in this study is the IP-free aerodynamic blade design test case described by Burton et al. [1]. This blade geometry is a CFD test case that is available to any worker. The flow exiting from the last stage blade is representative of modern designs. The last stage blade is 891mm long. The stator blade row has 60 blades and the rotor row has 65 blades. The geometry includes a blade tip gap of 4.2 mm so that the important effects of tip leakage on, for example, the separation from the flow guide [15], are captured in the calculations.

NUMECA's Autogrid5 and IGG were used to mesh the last stage blades. The mesh generated was a multi-block structured hexahedral mesh. y^+ values were kept below 10 so that boundary layers were fully resolved in the calculations without the need for wall-functions. 17 rows of cells were used across the rotor blade tip gap, so that the tip flow was fully resolved and the tip jet accurately captured in the simulations.

Vilmin [14] showed that at least 30 cells are needed in the tangential (θ) direction in order to correctly capture a blade passing frequency with the NLH method. This number must scale linearly with the number of harmonic frequencies that are calculated.

So, in a turbine stage calculation, if the number of blades in the stator and rotor blade rows are equal then at least 30N cells must be used in the θ-direction in the meshes on either side of the blade row interface. If, however, there are more rotor blades than there are stator blades, the pitch of the rotor blades will be less than that of the stator blades. So, the minimum number of cells needed in the mesh on the stator side of the interface has to be increased, to ensure that at least 30N cells are maintained across a rotor pitch distance in the stator blade row mesh. Conversely, the minimum number of θ-cells needed in the rotor blade row mesh will be reduced, because the circumferential length of the rotor blade row passage is less than the

Table 1. θ cell count scaling for harmonics

No. Harmonics	$\theta_{upstream}$	$\theta_{downstream}$	LSB Cell Count
1	35	31	812832
2	67	59	980464
3	99	83	1447148
4	131	111	1540848

stator blade pitch and 30N θ-cells per stator blade pitch can be achieved with less than this number of cells in the rotor mesh. The reverse argument is true for turbine stage calculations that feature more stator blades than rotor blades. In general, the number of cells needed in the θ-direction on either side of the stator-rotor interface will be weighted by the number of blades in the stator and rotor blade rows according to equations 4 and 5.

$$\theta_{cellsupstream} = 30N\frac{n_d}{n_u} \tag{4}$$

$$\theta_{cellsdownstream} = 30N\frac{n_u}{n_d} \tag{5}$$

The constraints on the minimum number of cells in the θ-direction described above results in the need for increasingly fine meshes as the number of harmonics calculated is increased. A preliminary benchmarking CFD exercise was carried out in order to verify that changes between results obtained with different numbers of harmonics, were principally caused by the change in the number of harmonics used and not by the accompanying change in mesh density. This involved generating meshes that were suitable for NLH calculations with between 1 and 4 harmonics, see Table 1, but running a steady-state calculation with a mixing plane coupling the rotor blade passage to the stator blade passage, in place of the NLH method. These calculations were carried out using NUMECA International Fine/TURBO 8.10 solver with the Low-Re Spalart-Allmaras turbulence model. The pitch-averaged boundary conditions for total pressure and three velocity components used on the stator inlet plane are shown in Figure 2. The rotor exit static pressure was set to 8800 Pa in all of the calculations. The working fluid was modelled as a perfect gas with fluid properties that are representative of wet steam. Convergence was achieved in less than 2000 iterations with a 3-level multi-grid and a CFL number equal to 3.

Figure 3 shows the radial variation of static pressure downstream of the rotor trailing edge. The meshes generated for modelling between 1 and 4 harmonics yield nearly identical results and any subsequent difference observed can only be due

to the number of harmonics modelled.

3.1.2 Exhaust Hood

The exhaust hood design used in the study was also the IP-free generic geometry defined as an open-access test case in Burton et. al [1]. Pointwise 16.04R5 was used to mesh the exhaust hood, with a multi-block hexahedral structured grid. The hood (diffuser) inlet plane was positioned at the same location as the rotor exit plane in the stage calculation, in order to avoid any need for interpolation in the coupling between the hood and stage calculations. It was not possible to generate a multi-block grid automatically with the meshing software used, but manual adjustment of the cell counts allowed the requirements for a 3 level multi-grid to be satisfied to accelerate convergence. The cell width at the wall was set to 0.1mm in order to give a y^+ of less than 10 for fully resolving the boundary layer without the use of wall functions. The final grid was mesh independent at 4.26 million cells.

3.2 Calculation Set-Up

3.2.1 Mixing Plane Approach

The single LSB passage was coupled to the exhaust hood by a mixing plane. The stator total pressure inlet was set as the same as the isolated stage calculation, with flow profiles as in Figure 2. The exhaust hood static pressure outlet was set at an average 10000Pa with back-flow control. The mass flow rate through the system was 88.7kg/s.

The working fluid configuration was set the same as the isolated stage calculation, with the water vapour modelled as a perfect gas with wet steam properties. A central spatial discretization was set as the numerical scheme.

Typically in CFD exhaust hood calculations, the turbulence is simulated by the k-ε turbulence model [16, 17] however in this application, the one equation eddy-viscosity Spalart-Allmaras turbulence model was selected to enable valid comparisons to be made to the NLH calculation results, as this is the most sophisticated turbulence model applicable with the NLH method in NUMECA Fine/TURBO 8.10.

The stage blocks were initialized with the converged isolated LSB steady calculation, described previously, to aid convergence. The exhaust hood flow field was initialized with a constant static pressure of 10000Pa and a temperature of 305K. The CFL number was set to 3 to reduce convergence times.

3.2.2 Non-Linear Harmonic Method

The calculation set up and initialization is mainly as described for the Mixing Plane calculation. The convergence rate and the coupling between mean flow and harmonics equations is improved when the flow-field is initialized by an existing quasi-steady solution. Subsequently, each calculation was started by running 1000 steady iterations before switching to a quasi-unsteady regime. Convergence was achieved after approximately 7000 iterations in total.

There are two main user selectable functions which are specific to the non-linear harmonic approach; number of perturbations (M) and number of harmonics per perturbation (N).

The number of perturbations (also called the number of blade passing frequencies per blade row) and is directly related

to the flow system geometry modelled. In the case of the exhaust hood system, given the periodicity of each row and the rotor speed of 3000rpm, the frequencies of perturbations associated with each harmonic are: [60; 65; 1] x 3000rpm = [3000Hz; 3250Hz, 50Hz] where 60 is the periodicity of the stator row, 65 of the rotor row and 1 of the exhaust hood [18]. The stator row sees one frequency of perturbation of 3250Hz from the downstream rotor row. The rotor row sees one frequency of perturbation of 3000Hz from the upstream stator row and one frequency of 50Hz from the downstream exhaust hood, i.e. two frequencies of perturbation. The exhaust hood sees one frequency of perturbation of the upstream rotor row of 3250Hz.

The number of harmonics modelled per perturbation directly effects the accuracy of the flow solution obtained. A balance must be made between the accuracy of the solution due to the increased number of harmonics, with the additional computational power required to solve them. Continuity over the domain interfaces improves with increasing number of harmonics [19]; capturing one harmonic (associated with the BPF) results in significant discontinuity whereas continuity is near perfect at N = 4. For engineering applications, the satisfactory continuity should be achieved with at least three harmonics [20]. To test this, the exhaust hood and coupled LSB calculation was run for between 1 and 4 harmonics, with the LSB cell count appropriate for the number of harmonics modelled, as shown in Table 1. Plotting the pressure recovery of the exhaust hood vs. the number of harmonics modelled in Figure 4 confirms that it is sufficient to model 3 harmonics per perturbation.

4 Results

In this section, results are compared for fully coupled exhaust hood and last stage blade flow predictions, that have been calculated using the NLH and mixing plane methods. This comparison allows the importance of modelling the circumferential asymmetry in the hood inlet/rotor exit flow to be assessed.

The widely adopted mixing plane approach allows the exhaust hood to be coupled to the last stage blades with a manageable computational demand. However, the exhaust hood's non axis-symmetric geometry and high swirl generates a circumferentially non-uniform back pressure from the exhaust hood onto the rotor. This is mixed out using mixing plane approach due to the circumferential averaging at the rotor-exhaust interface, resulting in unrepresentative conditions applied at rotor outlet.

Until now, the only known method to model this circumferential asymmetry was to model full rotor annulus in a frozen rotor or sliding mesh calculation, in order to achieve a periodic solution. The innovative treatment of the interface with the NLH approach as described in the work of Vilmin [14] enables both the time-averaged flow and the harmonics to be reconstructed either side of the interface even though only one blade passage is calculated.

4.1 Effect of Inlet Circumferential Asymmetry on the Exhaust Hood Flow Structure

Static pressure contours on the upstream side of the rotor-hood interface are shown in Figure 5 for flow solutions obtained using the NLH and mixing plane methods. The figure illustrates how circumferential non-uniformity is strongly coupled across the interface in the NLH calculations, and the impact of mixing out the non-uniformity in the mixing plane calculation. The novel treatment of the interface with the NLH method enables the non-uniformity present in the exhaust

Method	RMS_{P_t}	RMS_P
Mixing Plane Approach	140	41
Non-Linear Harmonic	776	645

Table 2. Rotor Outlet RMS Values [Pa]

hood flow to be transferred to the stage flow, generating a more representative boundary condition at the rotor outlet/hood inlet plane.

In order to quantify the level of non-uniformity present in the interface flow structure, a root mean square (RMS) metric was calculated according to equation 6 where U_n is the variable value calculated at the nth node on the interface plane, and n is the total number of interface nodes.

$$RMS_U = \sqrt{\frac{(U_1 - \bar{U})^2 + (U_2 - \bar{U})^2 + ...(U_n - \bar{U})^2}{n}} \tag{6}$$

The static and total pressure RMS values at the rotor outlet plane are tabulated in Table 2 for the solutions shown in Figure 5. The total pressure variation using the NLH approach is approximately 5 times that captured with the mixing plane method. The difference in static pressure variation between calculations is even more pronounced. Only radial variations in the flow are captured using the mixing plane method and so the higher values for the NLH calculation are a direct result of the additional circumferential variation in flow structure captured at the interface place using this method.

When comparing the flow structure within the exhaust hood, it is clear that both methods have accurately captured the high loss vortices, specifically the flow guide tip separation. The accurate modelling of the inlet asymmetry has a noticeable effect on the flow structure within the hood itself. Figure 6 shows that at the exhaust hood half joint plane, the asymmetry of the flow within the hood is reduced near the exhaust hood back wall with the non-linear harmonic approach.

The reduction in asymmetry is due to the swirl angle at inlet to the exhaust hood. The circumferential asymmetry of the swirl angle produced with the NLH approach works against the asymmetry in the exhaust hood. Figure 7 shows that there is a positive swirl angle on the underside of the hood inlet and a high negative swirl angle in the upper portion. This combination acts to reduce the asymmetry in the flow structure at the half joint plane.

4.2 Effect of Inlet Circumferential Asymmetry on the Exhaust Hood Static Pressure Recovery

The most widely used parameter in determining the performance of a steam turbine exhaust hood is the static pressure recovery coefficient, C_p, equation 7.

Method	C_p
Mixing Plane Approach	0.2725
Non-Linear Harmonic (NLH)	0.2479

Table 3. Exhaust hood static pressure recovery coefficients

-	Mixing Plane Approach	NLH	δ
P_t [Pa]	11217	11297	80
P [Pa]	9552	9588	32

Table 4. Rotor outlet average P at interface plane [Pa]

$$C_p = \frac{P_2 - P_1}{P_{T1} - P_1} = \frac{P_2 - P_1}{P_{dynamic_1}} \tag{7}$$

Table 3 compares the values of C_p calculated for the mixing plane NLH solutions described above. Despite the significantly different flow structure at the hood inlet plane calculated using the two methods, the static pressure recovery coefficients are surprisingly similar.

This was an unexpected result as the literature always stresses the importance of capturing the full blade row to exhaust hood coupling in calculations and experiments when investigating exhaust hood performance. In this case, using the NLH method results in a predicted pressure recovery that is just 3.3% lower than the value predicted using the mixing plane method, relative to the ideal case, C_p = 1.0.

The value of C_p depends upon three plane-averaged quantities i.e. total and static pressure on the hood inlet plane and the static pressure on the hood exhaust plane. The exhaust hood outlet static pressure was a fixed boundary condition of 10000Pa in both sets of calculations. Hence, any change in C_p between the two methods must result from changes in the total and static pressure fields at the hood inlet/rotor outlet boundary. Table 4 shows the difference between the mean pressure levels on the interface plane with the two approaches. The difference in mean total and static pressure is much smaller than the RMS levels (shown earlier in Table 2), and is only of order 10's Pa. It can therefore be concluded that even through the circumferential variations around on the hood inlet plane are significant compared to the radial flow variations, they do not have a large impact on the losses calculated within the exhaust hood for the geometry calculated in this paper.

It should be noted that predicting the accurate flow distribution is likely to be more important in design calculations of real exhaust hoods which include the internal structure of the hood. Local variations in the flow are important for the placement of internal support struts, splitter plates, bled-steam pipework etc. Large losses can potentially result if any of

these features are poorly designed with respect to the flow surrounding them. The idealised test case calculated in the present study does not feature any internal structure of this nature. It is therefore likely that a greater difference in C_p values would result from calculations with the different interface approaches, for real exhaust hood designs, with the internal hood structure included.

4.3 Effect of Diffuser Axial Length

A series of calculations were carried out in which the exhaust hood back wall was moved as shown in Figure 8. The aim of the calculations was to determine whether a tighter exhaust diffuser exit has any impact on the importance of circumferential variations in the hood inlet flow, on the value predicted for the exhaust hood pressure recovery coefficient, C_p. The back wall of the hood was moved to locations 50% and 75% of the distance from the diffuser outlet plane in the baseline hood design, for the calculations.

Additional mixing plane and NLH calculations were run with the back wall at the two new positions. The calculated pressure recovery coefficients are plotted against the diffuser axial length in Figure 9. 100% denotes the baseline diffuser length, described in the work of Burton [1].

Both methods shown the same trend of C_p with movement of the hood back wall position. As the diffuser exit becomes more constrained, the ability of the exhaust hood to recover pressure drops off rapidly. At the 75% position, some pressure recovery is still predicted, but at the 50% position the losses in the hood are much greater than any kinetic energy recovery in the diffuser. This results in an overall exhaust hood net loss ($C_p \leq 0$), causing the static pressure at rotor exit to increase to a level above that in the condenser. Hoznedl experimentally showed exhaust hood losses decrease with increasing axial length [21]. Also Finzel's extensive experimental study [22] showed that exhaust hood losses are relatively insensitive above a certain diffuser size, but below a critical level, losses significantly increase for more compact hoods, similar to the results shown in Figure 9.

The non-linear harmonic method consistently predicts a lower pressure recovery potential than with the mixing plane approach. As loss is a function of flow velocity cubed, any increase in flow non-uniformity (in this case the introduction of circumferential variations at the hood inlet plane with the NLH model) will be expected to result in higher predicted losses, as seen in Figure 9.

As the exhaust hood becomes more compact, the difference between the absolute values of pressure recovery predicted by the mixing plane approach and the NLH method can be seen to increase in Figure 9. However, the difference remains relatively small compared to the absolute value.

Figure 10 shows RMS_{P_T} and RMS_P around the rotor outlet plane for each back wall location. These results show how the circumferential variations in flow properties present in the NLH calculations, result in RMS variations that are an order of magnitude greater than in the mixing plane calculations, for all of the exhaust hood lengths calculated. This causes the lower values of Cp in the NLH predictions shown in Figure 9, for the reasons already discussed.

Although the predicted C_p does not dramatically change when modelling inlet circumferential variations with the NLH method, the inlet asymmetry has an important influence on the flow structure in the hood. The optimum placement of

splitter plates, bleed steam pipes and other hood internal 'furniture' is highly dependent on flow structure. These elements, if incorrectly located, can lead to large additional losses in real exhaust hood flows. The difference between C_p values calculated with the NLH and mixing plane methods would be expected to be much greater for real exhaust hoods, when the internal 'furniture' is included in the calculations. Figure 11 shows that $RMS_{P_{dyn}}$ at the diffuser exit plane is several times greater at 50% back wall location, compared to the result for the 100% position. Dynamic pressure is plotted as this essentially shows the velocity distribution at the diffuser outlet and it is the velocity field which is important to internal 'furniture' design and placement. The tighter diffuser exit at the 50% location leads to much larger gradients in the flow at this location, compared to the more generous 100% position, for the exhaust hood test case developed by Burton et al. [1]. It can be seen that the greater variation in the flow structure due to the inclusion of circumferential variations at diffuser inlet with the NLH approach, is carried over and effects the diffuser exit plane flow, at all back wall locations. This confirms that adopting the NLH method in place of a mixing plane approach will have an impact on the flow in the exhaust hood downstream of the diffuser, and supports the statements made previously concerning the potential for the NLH method to produce more accurate results for real exhaust hood flows, compared to the mixing plane method.

5 Conclusions

A novel application of the non-linear harmonic method has been used to enable a fully coupled LP last stage and exhaust hood flow calculation to be carried out, without the need to model the full rotor annulus. This treatment allows information on circumferential as well as radial flow variations to be transmitted across the interface between the stage calculation and the exhaust hood. The non-linear harmonic method has been shown to consistently predict slightly higher exhaust losses (lower values of pressure recovery coefficient, C_p) than similar calculations carried out using a mixing plane approach. The difference between predicted loss with the two methods increases for more compact hood designs, but still remains relatively small (a few percent) compared to the predicted absolute loss level. The exhaust hood geometry calculated was an idealised geometry with no internal structural features. Even though the circumferential coupling between the last stage and the hood flow did not have a large effect of exhaust hood loss, it was shown to have a significant impact on flow structure within the hood. It is therefore likely that the increased accuracy in predicted loss from adopting the non-linear harmonic method will have greater impact on real exhaust hood designs featuring internal exhaust 'furniture'. In these calculations any significant misalignment of the flow with features such as splitter plates etc, could have a large effect on the predicted overall hood loss.

References

[1] Burton, Z., Ingram, G. L., and Hogg, S., 2012. "A generic low pressure exhaust diffuser for steam turbine research". In ASME Turbo Expo, Copenhagen, Denmark, GT2012-68485.

[2] Liu, J., and Hynes, T. P., 2002. "The investigation of turbine and exhaust interactions in asymmetric flows: Part 2 - turbine-diffuser-collector interactions". In ASME Turbo Expo, Amsterdam, Netherlands, GT2002-30343.

[3] Benim, A., Geiger, M., Doehler, S., Schoenenberger, M., and Roemer, H., 1995. "Modelling the flow in the exhaust hood of steam turbines under consideration of turbine-exhaust hood interaction". *VDI BERICHTE,* **1185**, pp. 343–357.

[4] Fan, T., Xie, Y., Zhang, D., and Sun, B., 2007. "A combined numerical model and optimization for low pressure exhaust system in steam turbine". In ASME Power Conference, San Antonio, Texas, POWER2007-22147.

[5] Verstraete, T., Prinsier, J., Di Sante, A., Della Gatta, S., and Cosi, L., 2011. "Design optimization of a low pressure steam turbine radial diffuser usding an evolutionary algorithm and 3d cfd". In ASME Turbo Expo, GT2012-69515.

[6] Stanciu, M., Fendler, Y., and Dorey, J.-M., 2011. "Unsteady stator-rotor interaction coupled with exhaust hood effect for last stage steam turbines". In 9th European Turbomachinery Conference, B035.

[7] Li, Z., Li, J., Yan, X., Feng, Z., Ohyama, H., and Zhang, M., 2012. "Investigations on the flow pattern and aerodynamic performance of last stage and exhaust hood for large power steam turbines". In ASME Turbo Expo, Copenhagen, Denmark, GT2012-69291.

[8] Fu, J.-L., Liu, J.-J., and Zhou, S.-J., 2012. "Unsteady interactions between axial turbine and nonaxisymmetric exhaust hood under different operational conditions". *Journal of Turbomachinery,* **134**(4), p. 041002.

[9] Stanciu, M., Marcelet, M., and Dorey, J.-M., 2013. "Numerical investigation of condenser pressure effect on last stage operation of low pressure wet steam turbines". In ASME Turbo Expo, San Antonio, Texas, GT2013-94070.

[10] Megerle, B., McBean, I., Rice, T. S., and Ott, P., 2013. "Unsteady aerodynamics of low-pressure steam turbines operating under low volume flow". In ASME Turbo Expo, San Antonio, Texas, GT2013-95409.

[11] Beevers, A., Congiu, F., Pengue, F., and Mokulys, T., 2010. "An analysis of the merits of cfd for the performances prediction of a low pressure steam turbine radial diffuser". In ASME Turbo Expo, Glasgow, UK, GT2010-22107.

[12] Yoon, S., Stanislaus, F. J., Mokulys, T., Singh, G., and M., C., 2011. "A three-dimensional diffuser desing for the retrofit of a low pressure turbine using in-house exhaust design system". In ASME Turbo Expo, Vancouver, Canada, GT2011-45366.

[13] He, L. Ning, W., 1998. "Efficient approach for analysis of unsteady viscous flows in turbomachines". *American Institute of Aeronautics and Astronautics,* **36**(11), pp. 2005–2012.

[14] Vilmin, S., Lorrain, E., Hirsch, C., and Swoboda, M., 2006. "Unsteady flow modeling across the rotor/stator interface using the nonlinear harmonic method". In ASME Turbo Expo, Barcelona, Spain, GT2006-90210.

[15] Burton, Z., Ingram, G. L., and Hogg, S., 2013. "A generic steam turbine exhaust diffuser with tip leakage modelling and non-uniform hood outlet". In 11th European Turbomachinery Conference, Lappeenranta, Finland, ETC10-P38.

[16] Zhou, S., Liu, J., and Fu, J., 2007. "Experimental and numerical investigation of interaction between turbine stage and exhaust hood". *Proceedings of the Institution of Mechanical Engineers, Part A: Journal of Power and Energy,* **221**(7), pp. 991–999.

[17] Xu, X., Kang, S., and Hirsch, C., 2001. "Numerical simulation of the 3d viscous flow in the exhaust casing of a low-pressure steam turbine". In ASME Turbo Expo, GT2001-0487.

[18] Purwanto, A., Deconinck, T., Vilmin, S., Lorrain, E., and Hirsch, C., 2011. "Efficient prediction of nacelle installation effects at take-off conditions". In 9th European Turbomachinery Conference.

[19] He, L., Chen, T., Wells, R. G., Li, Y. S., and Ning, W., 2002. "Analysis of rotor-rotor and stator-stator interferences in multi-stage turbomachines". *Journal of Turbomachinery,* **124**(4), pp. 564–571.

[20] Hembera, M., Loos, A., Kahrmann, A., Danner, F., Kau, H., and Johann, E., 2006. "Validation of the non-linear harmonic approach for quasi-unsteady simulations in turbomachinery". In ASME Turbo Expo, Orlando, USA, GT2009-59933.

[21] Hoznedl, M., Tajc, L., Krejcik, J., Bednar, L., Sedlak, K., and Linhart, J., 2009. "Exhaust hood for steam turbines-single-flow arrangement". *Frontiers of Energy and Power Engineering in China,* **3**(3), pp. 321–329.

[22] Finzel, C., Schatz, M., Casey, M. V., and Gloss, D., 2011. "Experimental investigation of geometrical parameters on the pressure recovery of low pressure steam turbine exhaust hoods". In ASME Turbo Expo, Vancouver, Canada, GT2011-45302.

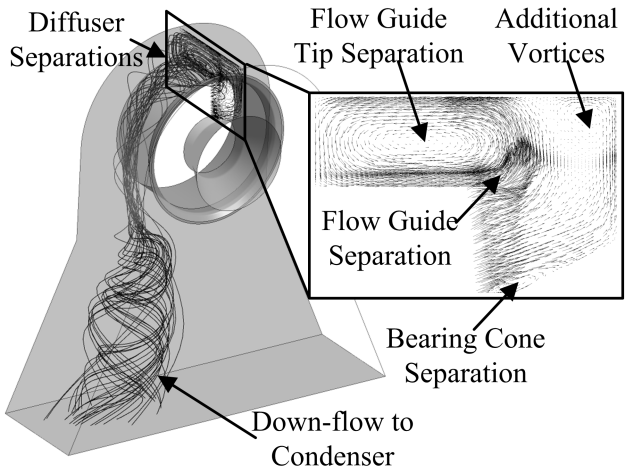

Fig. 1. Diffuser Outlet P_{dyn} RMS [Pa]

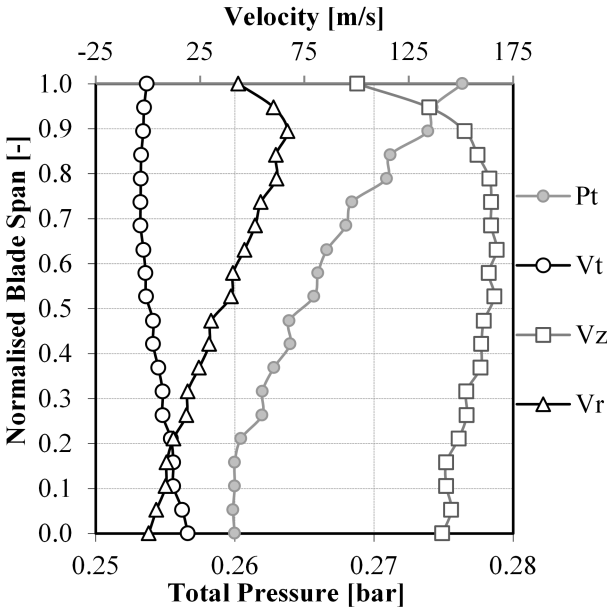

Fig. 2. Flow properties applied at stator inlet plane

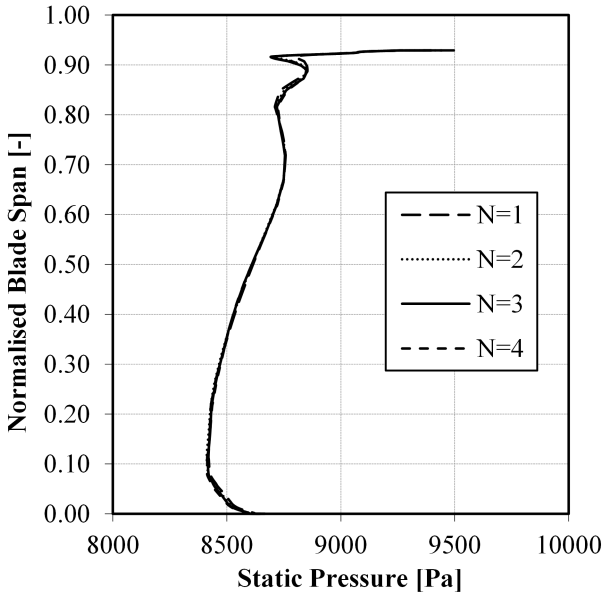

Fig. 3. P variations downstream of rotor trailing edge with cell count

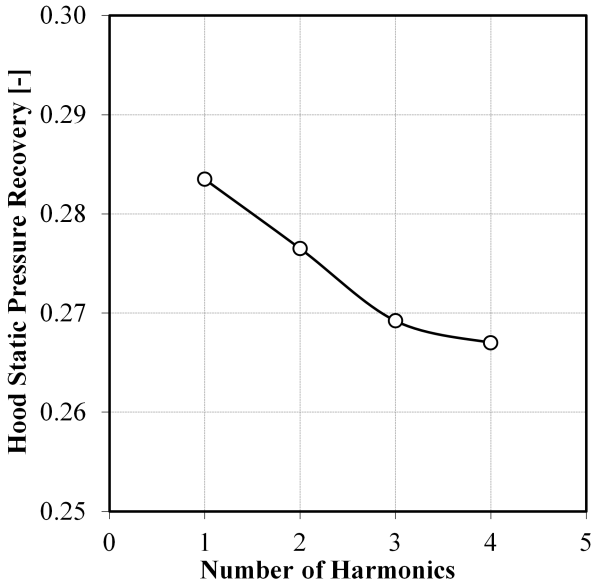

Fig. 4. Hood static pressure recovery coefficient variations with number of harmonics modelled

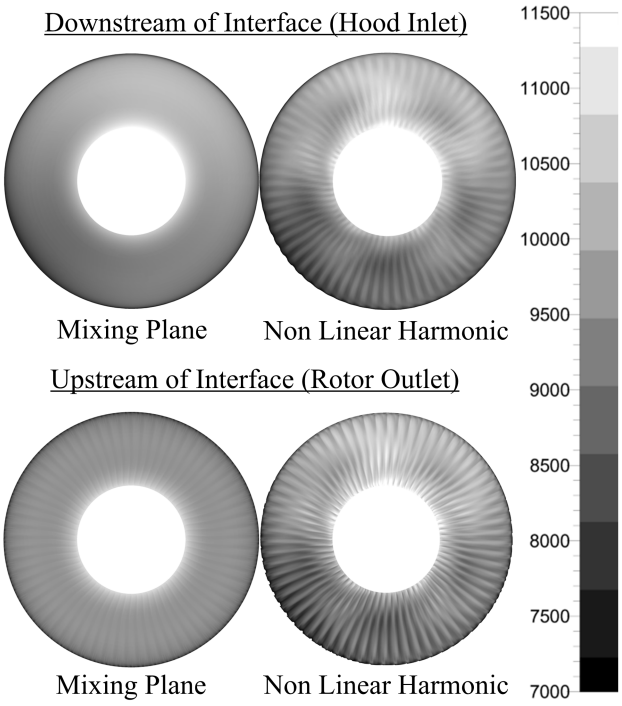

Fig. 5. P contours at rotor-hood interface [Pa]

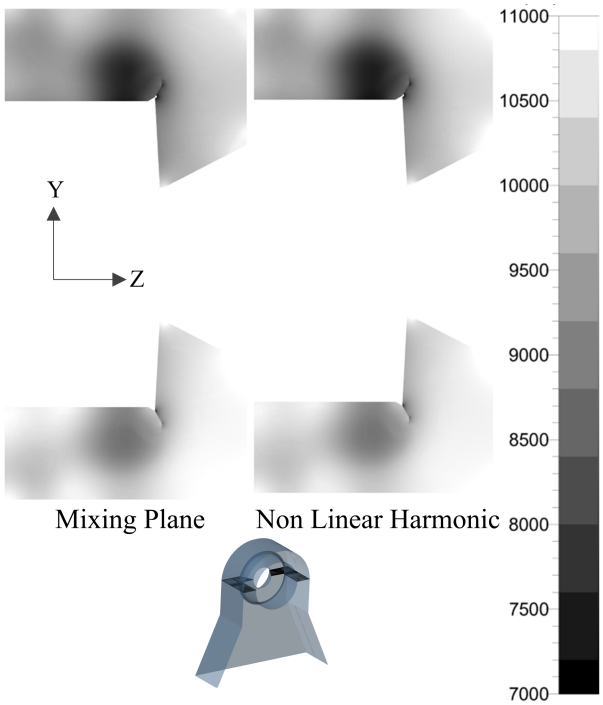

Fig. 6. P at the exhaust hood half-joint plane [Pa]

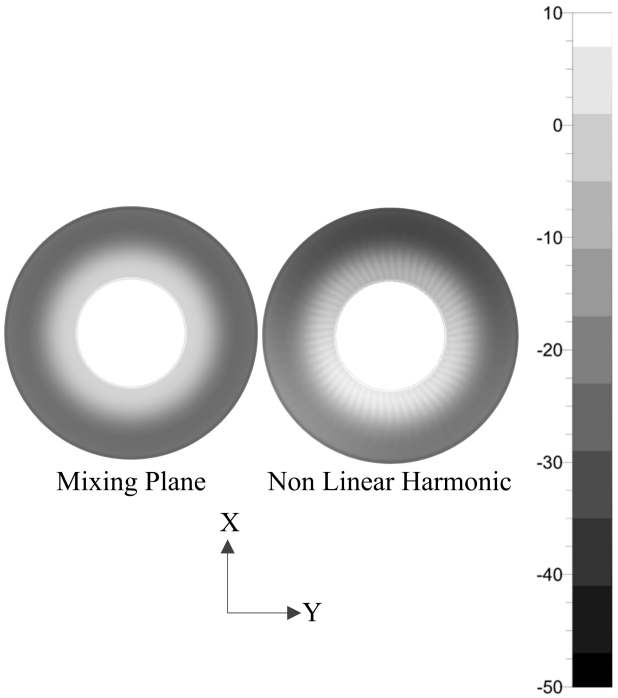

Fig. 7. Swirl angle at the hood inlet plane [^{o}]

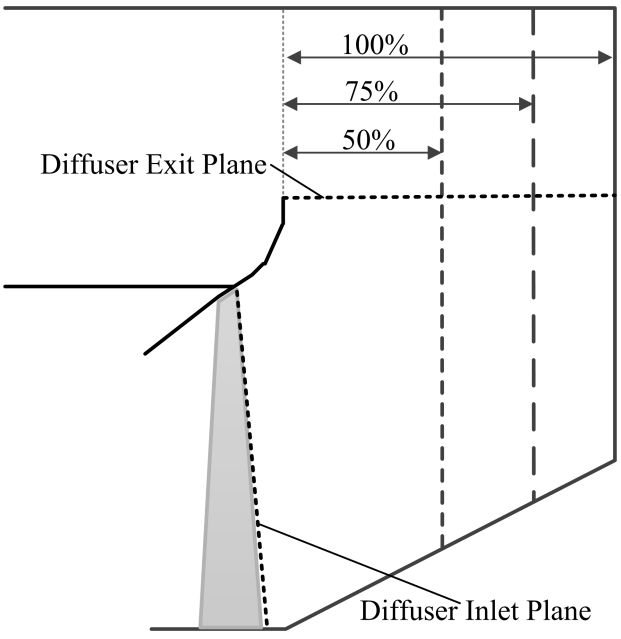

Fig. 8. Diagram of exhaust hood back wall locations

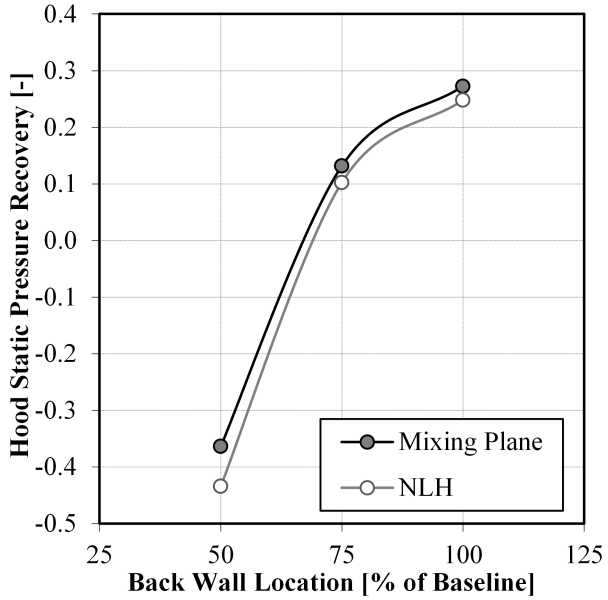

Fig. 9. Static pressure recovery coefficient vs. back wall location

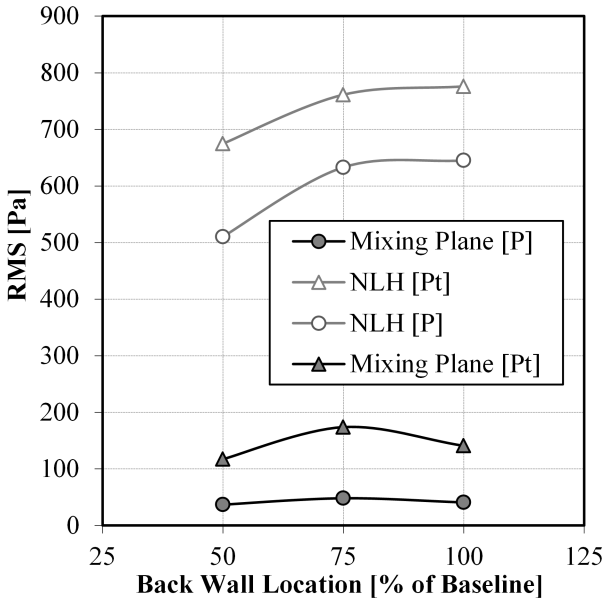

Fig. 10. Rotor Outlet P_{dyn} and P RMS [Pa]

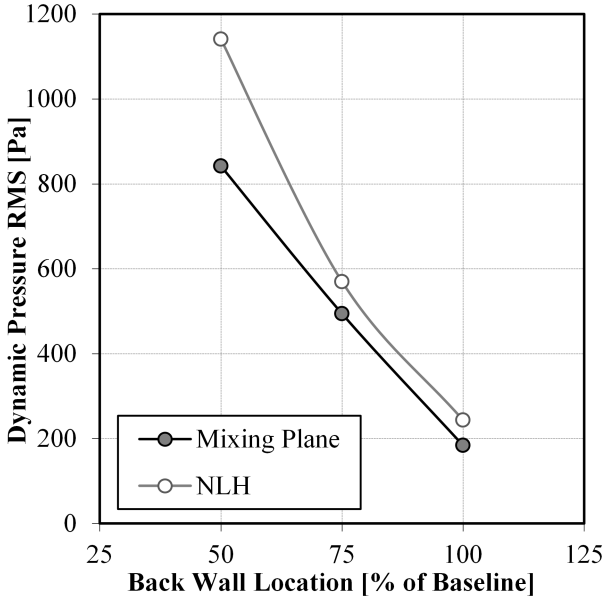

Fig. 11. Diffuser Outlet P_{dyn} RMS [Pa]